PERGAMON

International Journal of Heat and Mass Transfer 45 (2002) 4655–4661

International Journal of HEAT and MASS TRANSFER

www.elsevier.com/locate/ijhmt

Heat transfer characteristics of a two-phase closed thermosyphon to the fill charge ratio

Yong Joo Park [a,*], Hwan Kook Kang [b,1], Chul Ju Kim [a,2]

[a] Graduate School of Mechanical Engineering, Sungkyunkwan University, Chunchun-dong 300, Suwon 440-746, South Korea
[b] Research Team, Daehong Enterprise Co., #302 Daewoong Building, Yangpyungdong-4Ga 30, Seoul 150-104, South Korea

Received 8 August 2001; received in revised form 29 March 2002

Abstract

In this study, the heat transfer characteristics of a two-phase closed thermosyphon were investigated. For the test, a two-phase closed thermosyphon (copper container, FC-72 (C_6F_{14}) working fluid) was fabricated with a reservoir which could change the fill charge ratio. The experiments were performed in the range of 50–600 W heat flow rate and 10–70% fill charge ratio. Some findings are as follows.

The heat transfer coefficients of the evaporator to the fill charge ratio were nearly negligible. These presented about 1–5 kW/m^2 K with the increase of heat flux and compared with those of smooth surface, showed some enhancement by the grooved surface. However at the condenser, the heat transfer coefficients showed some enhancement with the increase of fill charge ratio by the expanded working fluid pool. And the heat transport limitations appeared in different ways to the fill charge ratio. For the relatively small fill charge ratio ($\Psi < 20\%$), it presented about 100 W (Ψ: 10%) by the dry-out limitation.

For the large fill charge ratio, it occurred by the flooding limitation and the maximum heat flow rate was about 500–550 W (*Bo*: 26–28), 230 W (*Bo*: 18.3) respectively and the Kutateladze number was about 1.9–2.1.

Keywords: Fill charge ratio; Heat transfer coefficient; Heat transport limitation; Dry-out; Flooding; Bond number; Kutateladze number

1. Introduction

A two-phase closed thermosyphon needs no wicks to return the condensate to the evaporator in the heat transport process because it uses gravity. However the evaporator must be positioned at the lower part than the condenser in the gravitation field. But because of its simple structure, stable operating condition during steady state, the characteristic of a thermal diode and wide operating temperature range, it was applied to many industrial fields. The applications of a two-phase closed thermosyphon were introduced first by Schmidt [1] in 1950s. In this study, it was found that the heat transport efficiency was very high although the temperature differences between evaporator and condenser were small. After then, there have been many researches in the different research topics [2–4]. In domestic, it was adopted for the cooling high power semiconductors (GTO Thyristor, IGCT, Diode etc.) in the Korea—High Speed Railway at the end of 1990s [5].

The analysis of two-phase flow heat transfer in a two-phase closed thermosyphon is very complicated. In this study, principally the analysis of the heat transfer characteristics to the fill charge ratio was performed. The condensation heat transfer in the condenser was based on the Nusselt (1916) model and compared with some correlations reported by Gross, Hahne, ESDU and

* Corresponding author. Tel.: +82-31-290-7474; fax: +82-31-290-5849.
E-mail addresses: y_j_park@hotmail.com (Y.J. Park), hkkang67@hanmail.net (H.K. Kang), cjkim@me.skku.ac.kr (C.J. Kim).
[1] Tel.: +82-2-2636-4027; fax: +82-2-2636-4026.
[2] Tel.: +82-31-290-7434; fax: +82-31-290-5849.

0017-9310/02/$ - see front matter
PII: S0017-9310(02)00169-2

Nomenclature

A	cross-section area (m^2)
Bo	Bond number, $D\left[\frac{g(\rho_l-\rho_v)}{\sigma}\right]^{1/2}$
C	constant
C_p	specific heat (J/kg K)
D	diameter (m)
g	acceleration of gravity (m/s^2)
h	heat transfer coefficient (W/m^2 K)
h_{lv}	latent heat of vaporization (J/kg)
j	volume flow rate per unit cross-section area (m/s)
k	thermal conductivity (W/m K)
K	Kutateladze number
L	length (m)
Nu^*	modified Nusselt number, $\frac{h}{k_l}\left[\frac{v_l}{g}\left(\frac{\rho_l}{\rho_l-\rho_v}\right)\right]^{1/3}$
p	pressure (N/m^2)
Pr	Prandtl number, v/α
Q	heat flow rate (W)
q	heat flux (W/m^2)
Re	Reynolds number
T	temperature (°C, K)
t	thickness (mm)
V	volume (m^3)
W	velocity (m/s)

Greek symbols

α	thermal diffusivity (m^2/s)
δ	liquid film thickness (mm)
μ	viscosity (kg/m s)
v	kinematic viscosity (m^2/s)
ρ	density (kg/m^3)
σ	surface tension (N/m)
φ	outer diameter (mm)
Ψ	fill charge ratio, V_l/V_e (%)

Subscripts

a	adiabatic, atmosphere
c	condenser
crit	critical
e	evaporator
f	fluid
k	Kutateladze
l	liquid
max	maximum
s	solid
sat	saturation
t	total
v	vapor
w	wall, Wallis

Uehara et al. [6]. While in the evaporator, the nucleate boiling model made by Roshenow [7] was applied to predict the heat transfer coefficients. And compared with the correlation suggested by Immura et al. [8].

For the heat transport limitations to the fill charge ratio, Improved Cohen and Bayley model [2,12] illustrating the relationships between the fill charge ratio and the critical heat flux at the dry-out limitation was adopted. While for the large fill charge ratio, Eq. (14) and correlation that Faghri et al. [9] improved the existing correlations to predict the flooding limitation including the effects of diameters and properties of working fluids.

2. Heat transfer coefficient

2.1. Evaporator

The heat transfer mechanisms at the evaporator occur in various patterns that are the natural convection, the evaporation, the nucleate boiling and the combination of each ones to the fill charge ratio and the heat flux etc. [10]. For a small fill charge ratio, the convective boiling and the evaporation at the condensate film returning to the evaporator is a dominating heat transfer mechanism. However as the fill charge ratio increases the nucleate boiling dominates the heat transfer mechanism at the evaporator.

In this study, the heat transfer coefficient at the evaporator was based on the nucleate boiling in the working fluid pool. In 1962, Rohsenow [7] reported the model of the nucleate boiling like Eq. (1). In Eq. (1), substitute Eq. (2) for $[\overline{T_e} - T_v]$ and then rearranging yields Eq. (3).

$$\frac{q}{\mu_l h_{lv}}\left[\frac{\sigma}{g(\rho_l-\rho_v)}\right] = \left(\frac{1}{C_{sf}}\right)^{1/r} Pr_l^{-s/r}\left[\frac{C_{p,l}[\overline{T_e}-T_v]}{h_{lv}}\right]^{1/r} \tag{1}$$

where $r = 0.33$, $s = 1.7$ and C_{sf} is the solid–fluid constant.

$$q = \overline{h_e}[\overline{T_e} - T_v] \tag{2}$$

$$\overline{h_e} = \left(\frac{q}{h_{lv}}\right)^{0.67}\left[\mu_l \Big/ \sqrt{\frac{\sigma}{g(\rho_l-\rho_v)}}\right]^{0.33}\frac{C_{p,l}}{C_{sf}}\frac{1}{Pr_l^{1.7}} \tag{3}$$

And the correlation reported by Immura et al. [8] was also compared with the experimental data.

$$\overline{h_e} = 0.32\left(\frac{\rho_l^{0.65}k_l^{0.3}C_{p,l}^{0.7}g^{0.2}q^{0.4}}{\rho_v^{0.25}h_{lv}^{0.4}\mu_l^{0.1}}\right)\left(\frac{p_{sat}}{p_a}\right)^{0.3} \tag{4}$$

2.2. Condenser

At the condenser of a two-phase closed thermosyphon, the filmwise condensation occurs. Nusselt (1916) derived the heat transfer coefficient of the laminar filmwise condensation on a vertical plate. The correlation is as follows.

$$\overline{h_c} = 0.943\left\{\frac{\rho_l g k_l^3(\rho_l-\rho_v)[h_{lv}+0.68C_{p,l}(T_v-\overline{T_c})]}{\mu_l L_c(T_v-\overline{T_c})}\right\}^{1/4} \tag{5}$$

Eq. (5) can be expressed in the dimensionless form, Eq. (6).

$$\overline{Nu_c^*} = \frac{\overline{h_c}}{k_l}\left[\frac{v_l^2}{g}\left(\frac{\rho_l}{\rho_l-\rho_v}\right)\right]^{1/3} = 0.925Re_{max,l}^{-1/3} \quad (Re_{max,l}<325) \tag{6}$$

where $Re_{max,l} = (\overline{w}_{max,l}\delta_{max}/v_l) = (Q/\pi D\mu_l h_{lv})$ (at the adiabatic section).

Uehara et al. [11] gave the following correlations based on their experimental data for a filmwise condensation on a vertical plate.

Wavy-laminar range

$$\overline{Nu_c^*} = 0.884Re_{max,l}^{-1/4} \quad (0.5 < Re_{max,l} < 325Pr_l^{-0.96}) \tag{7}$$

Turbulent range

$$\overline{Nu_c^*} = 0.044Pr_l^{2/5}Re_{max,l}^{1/6} \quad (Re_{max,l} > 325Pr_l^{-0.96}) \tag{8}$$

Gross [12] also gave the following equation.

$$\overline{Nu_c^*} = \left[(0.925f_pRe_{max,l}^{-1/3})^2 + (0.044Pr_l^{2/5}Re_{max,l}^{1/6})^2\right]^{1/2} \tag{9}$$

where $f_p = [1-0.63(p^*)^{3.3}]^{-1}$: enhancement factor. p^* is the ratio of the pressure within the thermosyphon to the critical pressure of the working fluid. The experimental data in this study were calculated by Eq. (10) and compared with the above equations.

$$\overline{h_c} = \frac{q}{[T_v-\overline{T_c}]} \tag{10}$$

3. Heat transfer limitation

3.1. Dry-out limitation

In the heat transfer limitation of a two-phase closed thermosyphon, the dry-out limitation occurs for the fill charge ratio is relatively small. The condensate falls down along the wall and reaches at the evaporator. The condensate starts evaporating and boiling by the input power and as more and more to the bottom, the thickness of the condensate film is thinner. Eventually dries out, so the wall temperature rises from the bottom of the evaporator at the limitation.

For the dry-out limitation, Improved Cohen and Bayley model [13] that illustrated the relationship between the fill charge ratio and the heat flux was adopted.

$$\left(\frac{q_{crit}}{\rho_v h_{fg}}\right)\left[\frac{\sigma g(\rho_l-\rho_v)}{\rho_v^2}\right]^{-1/4} = \left[\frac{g\rho_l^2(D_c/D_e)}{3\mu L_e\sqrt[4]{\sigma g\rho_v^2(\rho_l-\rho_v)}}\right] \times \left[\frac{V_t/\pi D_c}{4L_c/5+L_{ac}+(D_e/D_c)^{2/3}(L_{ac}+3L_e/4)}\right]^3 \times \left[\frac{V_e/V_t(V_l/V_e)-\rho_v/\rho_l}{1-\rho_v/\rho_l}\right]^3 \tag{11}$$

Shiraishi et al. [13] showed that the correlation, Eq. (11) agreed with the experimental data in their experiments and now also the Eq. (11) was used for this study.

3.2. Flooding limitation

Faghri et al. [9] considered the effects of the diameter of the container and the properties of the working fluid to predict the flooding limit of a two-phase closed thermosyphon. In this study, the flooding limitation was suggested to the Bond number.

Wallis [14] and Kutateladze [15] suggested the following correlations for the flooding limitation.

$$j_v^{*1/2} + mj_l^{*1/2} = C_w \tag{12}$$

where $j_i^* = j_i\rho_i^{1/2}[gD(\rho_l-\rho_v)]^{-1/2}$

$$K_v^{1/2} + K_l^{1/2} = C_k \tag{13}$$

where $K_i = j_i\rho_i^{1/2}[g\sigma(\rho_l-\rho_v)]^{-1/4}$

In Eqs. (12) and (13) $j_i = ((Q/h_{lv})/\rho_i A)$, $i = l, v$

Wallis (1961) reported that at flooding limitation, the value of j_v^* is 1($j_l^* = 0$) and for most cases to the open system, the value of m is 1 and the value of C_w is 0.8–1. Pushkina and Sorokin [16] suggested that the value of K_v is 3.2 ($C_k = 3.2^{1/2}$).

Wallis and Makkenchery [17] introduced the effect of diameter at the flooding limit and suggested the following correlation.

$$\frac{C_k}{C_w} = Bo^{1/4} \tag{14}$$

Faghri et al. [9] developed this correlation and proposed the following correlation for other working fluids besides water.

$$C_k^2 = K = \left(\frac{\rho_l}{\rho_v}\right)^{0.14}\tanh^2 Bo^{1/4} \tag{15}$$

and also proposed the following correlation for maximum heat rate by flooding limitation.

$$Q_{\max} = Kh_{\mathrm{lv}}A[g\sigma(\rho_{\mathrm{l}} - \rho_{\mathrm{v}})]^{1/4}\left[\rho_{\mathrm{v}}^{-1/4} + \rho_{\mathrm{l}}^{-1/4}\right]^{-2} \quad (16)$$

In this Eq. (16), the cross-section area, A has the parameter of a diameter, D. So it can be rewritten as follows.

$$Q_{\max} = \frac{\pi K h_{\mathrm{lv}}}{4} Bo^2 \frac{\sigma^{5/4}}{[g(\rho_{\mathrm{l}} - \rho_{\mathrm{v}})]^{3/4}}\left[\rho_{\mathrm{v}}^{-1/4} + \rho_{\mathrm{l}}^{-1/4}\right]^{-2} \quad (17)$$

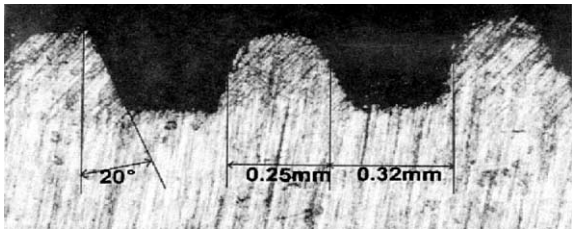

Fig. 2. Microscopic view of the two-phase closed thermosyphon grooves.

4. Experimental apparatus and method

4.1. Two-phase closed thermosyphon

Fig. 1 shows the configuration of the two-phase closed thermosyphon and the locations of thermocouples for present study (also see Fig. 2). It is the same geometry as the ones that were adopted for the cooling semiconductors of the main power transition system in the Korea—High Speed Railway. As you can see, it was made of a copper tube container, the FC-72 (C_6F_{14}) working fluid and fabricated with a working fluid reservoir that can change the fill charge ratio by the high vacuum sealed valve. Table 1 shows the specifications of the two-phase closed thermosyphon for the present test in detail with two two-phase closed thermosyphons that have different geometries. The thermocouples (φ: 0.12 mm, T-type) for the axial wall temperature distributions were attached on the outer wall of the two-phase closed thermosyphons by welding. For the measurement of vapor temperature, two thermocouples (φ: 1 mm, K-type) were inserted in the evaporator and the condenser respectively.

4.2. Experimental apparatus

Fig. 3 shows the schematic diagram of experimental apparatus. As you can see, an electric resistance wire (φ: 0.4 mm, Ni–Cr) was wound uniformly round the outer wall of the evaporator to supply the power that was supplied by the DC AVR (1 kW) and the power was checked by the precision meter (Yokogawa-WT110). The two-phase closed thermosyphon was surrounded

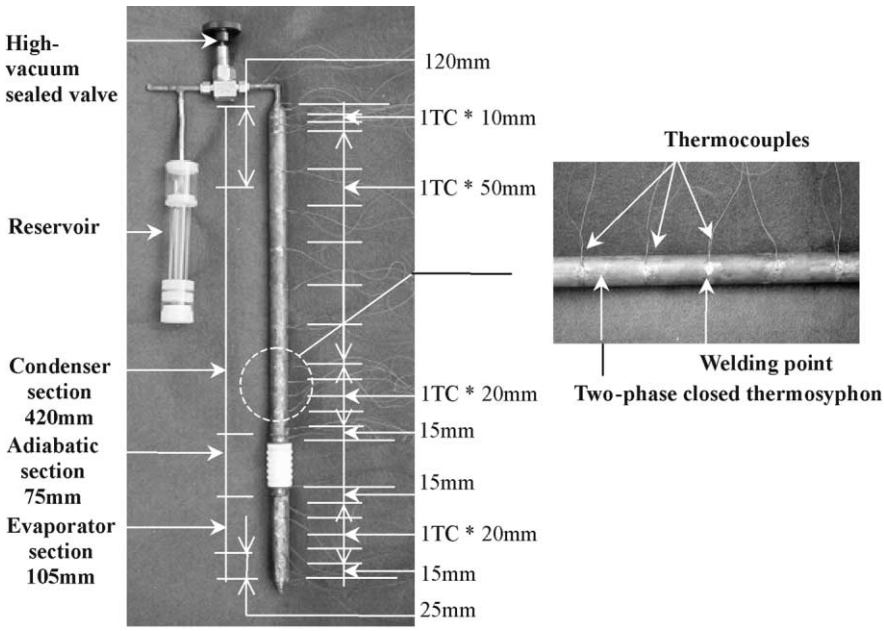

Fig. 1. Configuration of the two-phase closed thermosyphon and locations of thermocouples.

Table 1
The specifications of two-phase closed thermosyphons for present study

	A (grooved surface)		B (smooth surface)		C (grooved surface)
Structure of inner surface	Helical groove Helix angle: 18° Thickness: 0.32 mm Depth: 0.28 mm Fin thickness: 0.25 mm Number: 130 EA		Smooth		Helical groove The same as A The same as A The same as A The same as A Number: 80 EA
		Evaporator	Adiabatic	Condenser	Evaporator, Adiabatic, Condenser
Container	Length	105 mm	75 mm	420 mm	The same as A, B
	Outer diameter material	22.23 mm	32.7 mm	22.23 mm	Outer diameter: 15.88 mm
	Material	Copper	Ceramic	Copper	
Working fluid	PFC (C_6F_{14})				
Fill charge ratio	10–70%				70%

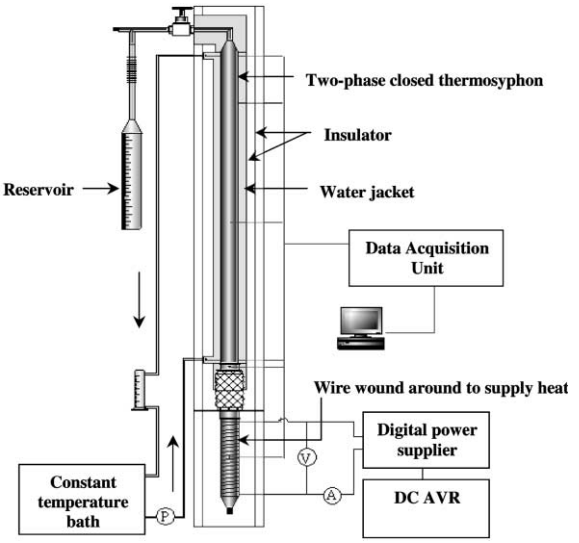

Fig. 3. Schematic diagram and the experiments apparatus for the test.

with insulators of the glass wool (t: 20 mm) and the polyethylene to stop the heat transfer to the environment. For the cooling of the condenser, the cold water was circulated from the constant temperature bath through the water jacket. During the test, the vapor temperature was constant at 50 °C by adjusting the coolant temperature to the power. A series of tests were performed to the change of the fill charge ratio from 10% to 70% by 10% and every 50 W of heat flow rate was supplied step by step from 50 W to the limitation. The heat transport limitation was defined as the temperature of evaporator increased continuously not keeping the constant value in 5–10 min.

5. Results and discussion

5.1. Heat transfer coefficient

Fig. 4 shows the heat transfer coefficients of the evaporator. As you can see, for the smooth surface, in about 4–80 kW/m^2 heat flux the heat transfer coefficient presented about 0.7–2 kW/m^2 K. And they were in good agreement for in Rohsenow's pool boiling model, Eq. (3) the value of constant, C_{sf} was about 0.004. The effect of the fill charge ratio seemed to be negligible. While for the grooved surface, the heat transfer coefficient presented about 2–4 kW/m^2 K. It also showed that the effect of the fill charge ratio was nearly negligible.

Fig. 5 shows the variations of modified Nusselt number versus the maximum Reynolds number of the condensate at the condenser. As shown in the picture, for the smooth surface, the correlation reported by Gross [12] was in good agreement with the experimental data. And the heat transfer coefficient presented some

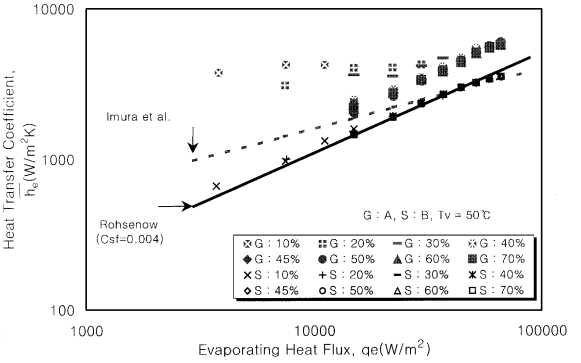

Fig. 4. Heat transfer coefficient versus heat flux at the evaporator for various fill charge ratio.

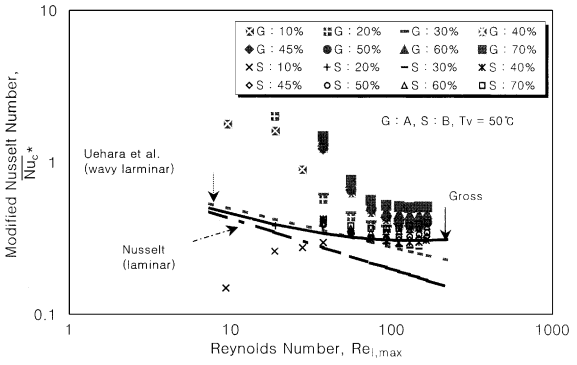

Fig. 5. Nusselt number versus Reynolds number at the condenser for various fill charge ratio.

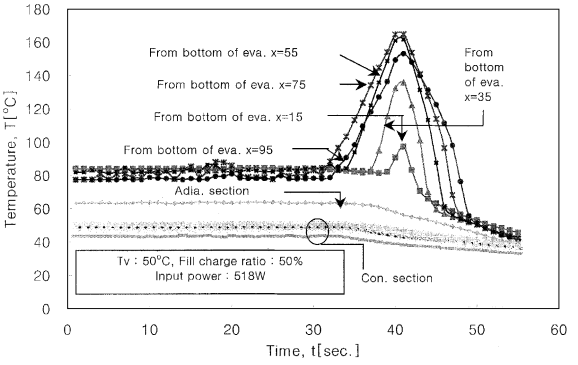

Fig. 7. Wall temperature variations of the two-phase closed thermosyphon along the axial distance at flooding limit (For A).

enhancement with the increase of the fill charge ratio for both of the smooth and the grooved surface. It can be explained that during the steady state, the heat transfers directly from the high temperature working fluid pool [18] expanded up to the lower part of the condenser to the condenser without evaporating process.

5.2. Heat transfer limit

Figs. 6 and 7 show the wall temperature distributions along the two-phase closed thermosyphon at the limitation. Fig. 6 shows the characteristics of temperature distribution at the dry-out limitation (Ψ: 10%). At 15, 35 mm from the bottom of the evaporator, the temperature first increased and then the others ($x = 55$, 75, 95 mm) did. At the dry-out limitation, the condensate film thickness dries thinner down to the lower part of the evaporator and then eventually dries out. So the temperature increases from the bottom of the evaporator. While for the large fill charge ratio (Ψ: 50%), the heat transport limitation occurred by the flooding phenomena by the shear stress at the interface between the condensate flow and the uprising vapor flow. So the dry-out by the flooding occurred at the top of the evaporator where the vapor velocity was maximum. Fig. 7 shows these phenomena exactly. Fig. 8 shows the critical heat flux versus the fill charge ratios. In this figure, the experimental data showed some agreements with Improved Cohen and Bayley model for the dry-out limit. Over the fill charge ratio 20%, it showed a weak relationship between the critical heat flux and the fill charge ratio. In addition to over 40%, it showed nearly constant value. Figs. 9 and 10 show Kutateladze number and heat transport limitation versus Bond number at the flooding limitation. As you can see, for the $Bo = 18.2$ and 27.6, K presented 1.6 and 1.9 respectively. And the variations of K were similar to the correlation of Tien and Chung.

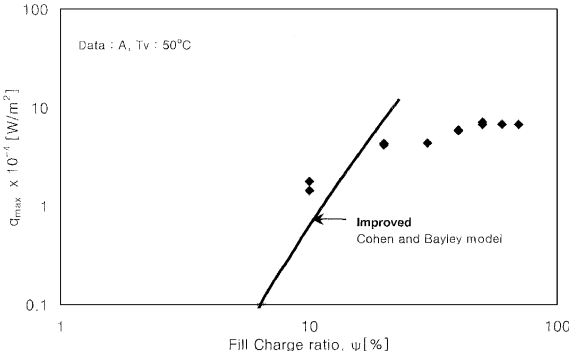

Fig. 8. Critical heat flux versus fill charge ratio.

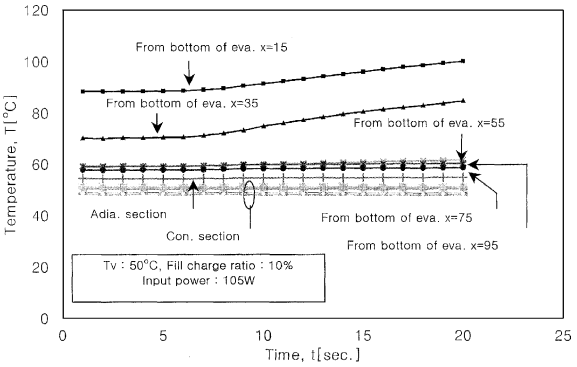

Fig. 6. Wall temperature variations of the two-phase closed thermosyphon along the axial distance at dry-out limit (For A).

In Fig. 10, the flooding limitations are shown compared with the Eq. (14). For the $Bo = 18.2$ and 27.6, Q_{max} presented about 180 and 500 W respectively. And the experimental data showed a good agreement with Wallis's correlation at $C_w = 0.8$.

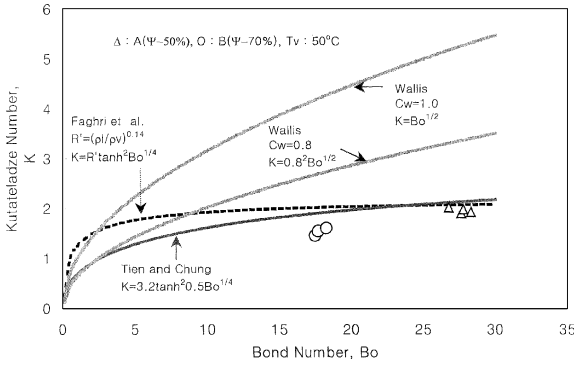

Fig. 9. Kutateladze number versus Bond number at the flooding limit.

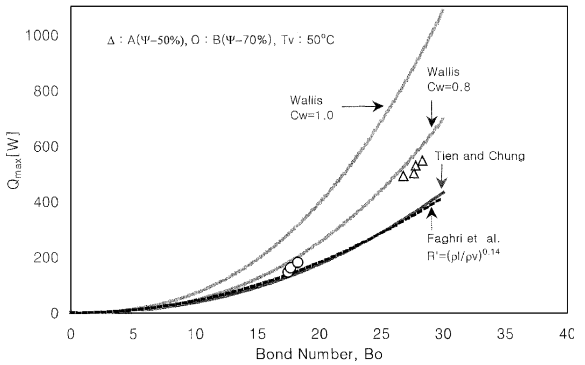

Fig. 10. The maximum heat rate versus Bond number at the flooding limit.

6. Conclusions

In this study, the heat transfer characteristics of a two-phase closed thermosyphon to the fill charge ratio were investigated. Several tests were performed and the results were compared with the existing correlations. The conclusions from the present study are as follows.

1. The heat transfer coefficient of the evaporator showed a trend that increased with the increase of the power. And the effect of the fill charge ratio was nearly negligible for both of the smooth surface and the grooved surface. For the smooth surface, the experimental data generally showed a good agreement with the correlation reported by Rohsenow and the value of the constant, C_{sf} was about 0.004. At the condenser, the trend of modified Nusselt number was shown as decrease with the increase of Reynolds number. And it showed some enhancement with the increase of the fill charge ratio because the working fluid pool in the evaporator expands up to the lower part of the condenser.

2. The heat transport limitations occurred in different ways to the fill charge ratio. For the small fill charge ratio ($\Psi < 20\%$), it occurred by the dry-out limitation and the temperature of the evaporator arose from the bottom of the evaporator. While for the large fill charge ratio, it occurred by the flooding limitation. And the temperature of the evaporator arose from the top of the evaporator. At the flooding limitation, for the $Bo = 18.2$ and 27.6, Q_{max} presented about 180 and 500 W respectively. And the experimental data showed a good agreement with Wallis's correlation at $C_w = 0.8$.

References

[1] E. Schmidt, in: Proc. Instn. Mech. Engrs., Conf. ASME, London, 1951, pp. 361–363.
[2] H. Cohen, F.J. Bayley, Heat transfer problems of liquid-cooled gas-turbine blades, Proc. Instn. Mech. Engrs. 169 (1955) 1063–1074.
[3] J.C. Charto, W.T. Laurence, Development Heat Transfer, 1964, pp. 371–388.
[4] Larkin, An experimental study of two-phase thermosyphon tube, Trans. CSME 4 (1971) 17–24.
[5] C.J. Kim, W.K. Kang, J.S. Lee, Y.J. Park, Design and manufacturing of the heat sink using heat pipes, Hyundai Heavy Industry Co., Report, 1997–2000 (in Korean).
[6] A. Faghri, Heat Pipe Science and Technology, Taylor & Francis, London, 1995, pp. 341–376.
[7] W.M. Rohsenow, A method of correlating heat transfer data for surface boiling of liquids, Trans. ASME 84 (1962) 969–1962.
[8] Immura et al., Heat Trans.-Jpn. Res. 2 (1979) 41.
[9] A. Faghri, M.M. Chen, M. Morgan, Heat transfer in two-phase closed conventional and concentric annular thermosyphon, Int. J. Heat Mass Trans. 111 (1989) 611–618.
[10] P. Van Carey, Liquid–Vapor Phase Change Phenomena, Hemisphere, Washington, DC, 1992, pp. 215–298.
[11] H. Uehara, H. Kusuda, T. Nakaoka, A. Yamada, Filmwise condensation for turbulent flow on a vertical plate, Heat Trans.-Jpn. Res. 12 (2) (1983) 85–96.
[12] U. Gross, Reflux condensation heat transfer inside a closed thermosyphon, Int. J. Heat Mass Transfer 35 (2) (1992) 279–294.
[13] M. Shiraishi, M. Yoneya, A. Yabe, Visual study of operating limit in the two-phase thermosyphon, in: Proc. 5th Int. Heat Pipe Conf., 1984, pp. 11–17.
[14] G.B. Wallis, Flooding velocities for air and water in vertical tubes, AEEW-R123, 1961.
[15] S.S. Kutateladze, Elements of hydrodynamics of gas–liquid systems, Fluid Mech.-Soviet Res. 14 (1972) 29–50.
[16] O.L. Pushikina, Y.L. Sorokin, Breakdown of liquid film motion in vertical tubes, Heat Trans.-Soviet Res. 1 (5) (1969) 56–64.
[17] G.B. Wallis, S. Makkenchery, The hanging film phenomenon in vertical annular two-phase flow, J. Fluids Eng. 3 (1974) 297–298.
[18] M.S. El-Genk, H.H. Saber, Determination of operation envelops for closed two-phase thermosyphons, Int. J. Heat Mass Transfer 42 (1999) 889–903.